

2  
Presented at the Joint Meeting of the  
International Association for the Advancement of High Pressure Science and Technology  
and the  
American Physical Society Topical Group on Shock Compression of Condensed Matter  
June 28 - July 2, 1993

Conf 1996 26 - 40

## TIME-RESOLVED SHOCK COMPRESSION OF POROUS RUTILE: WAVE DISPERSION IN POROUS SOLIDS

M. U. Anderson, R. A. Graham, and G. T. Holman  
Sandia National Laboratories, Albuquerque, New Mexico 87185-5800

Rutile ( $TiO_2$ ) samples at 60% of solid density have been shock-loaded from 0.21 to 6.1 GPa with sample thickness of 4 mm and studied with the PVDF piezoelectric polymer stress-rate gauge. The technique uses a copper capsule to contain the sample which has PVDF gauge packages in direct contact with the front and rear surfaces. A precise measure is made of the compressive stress wave velocity through the sample, as well as the input and propagated shock stress. The initial density is known from the sample preparation process, and the amount of shock-compression is calculated from the measurement of shock velocity and input stress. Shock states and re-shock states are measured. The observed data are consistent with previously published high pressure data. It is observed that rutile has a "crush strength" near 6 GPa. Propagated stress-pulse rise times vary from 234 to 916 nsec. Propagated stress-pulse rise times of shock-compressed HMX,  $2Al + Fe_2O_3$ ,  $3Ni + Al$ , and  $5Ti + 3Si$  are presented.

### INTRODUCTION

Shock compression of highly porous rutile ( $TiO_2$ ) has been investigated with a time-resolved shock compression technique. The rutile material was chosen to: (1) develop an understanding of a highly porous single component system under shock compression, and fully qualify the time-resolved shock compression technique, (2) provide data for the extensive numerical simulation data base on rutile<sup>1</sup>, (3) compare with the information learned through previous sample preservation (recovery) work on rutile<sup>1</sup>, and (4) compare with the existing high pressure shock compression work on rutile as reported by Bugaeva et al.<sup>2</sup> The present work is part of an overall study of shock-induced solid state chemistry.<sup>3-5</sup>

### EXPERIMENTAL TECHNIQUE

The time-resolved shock compression technique used in the present study subjects the powder sample to controlled shock-loading from either a compressed-gas gun, or high explosive loading.<sup>6</sup> The sample was encased in a copper capsule with PVDF<sup>7</sup> gauge packages at both input and propagated locations as in Figure 1. High explosive loading is described in Holman's<sup>8</sup> paper in the present proceedings.

The material used in the present study was "Puratronic" grade, high purity powder from Johnson-Matthey. Particle sizes range from 1 - 800  $\mu m$ . Powder samples were pressed to 60% of  $4.26 \text{ gm/cm}^3$ . Difficulty was encountered when pressing the samples due to the high crush strength of rutile, consistent with shock-compression observations.

#### Sample Preparation

The powder samples were pressed directly into the instrumented copper capsule to achieve intimate

contact at the PVDF gauge package/sample interface. The piezoelectric polymer PVDF measures stress-rate directly and is sensitive to sample imperfections such as density gradients, or  $\mu m$  size voids at the PVDF interface.

The powder samples were pressed in three uniform layers using a tool steel die at sample pressures of 500 MPa for each layer. The copper containment ring began to expand radially at sample pressures above 350 MPa unless externally supported. Sample densities achieved averaged 59.5%,  $\pm 0.9\%$ .

At shock-pressures below 2 GPa, the PVDF/sample impedance mismatch required use of a buffer material to isolate the front and rear surfaces of the sample from the copper. The polymer TPX was chosen to impedance match the rutile at low pressure. During the sample compaction process, the TPX was observed to compress by 10% at 500 MPa sample pressure, changing the TPX buffered sample to 56.8% dense, with a sample thickness uncertainty of  $\pm 75 \mu m$ .

The experimental arrangement as shown in Figure 1, consists of a powder sample encased in a copper capsule with PVDF gauge packages at both input and propagated locations. A precise measure is made of the compressive stress-wave velocity through the sample, as well as the input and propagated stresses. The initial density is known from the sample preparation process, and the amount of shock-compression is calculated from measurement of wave velocity and input stress.

The conservation of momentum assumption used in the calculation is known to be violated by observation of the propagated wave dispersion. The pressure-versus-relative volume states identified using this technique provide a reasonable measure of material response under shock compression even though the exact volume is not identified.

MASTER

DISTRIBUTION OF THIS DOCUMENT IS UNLIMITED

875

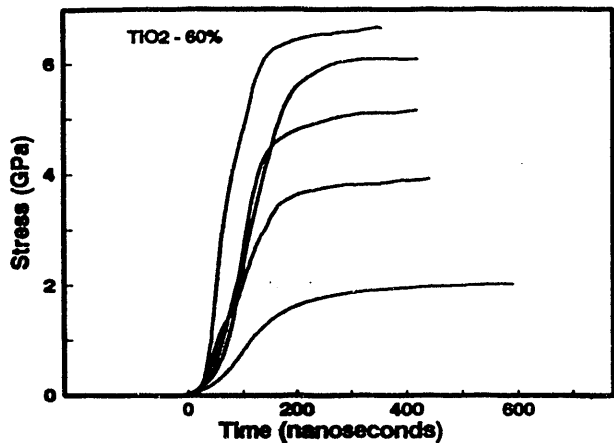


Figure 2. The dispersed structure of an input shock propagated through 4mm of 60% dense rutile shows risetime increasing inversely with stress.

The shock-compression behavior of 60% dense rutile shows a high crush strength with a well-defined path toward solid density that shows good agreement with existing high pressure data.

The pressure-versus-relative volume data are shown in Figure 3 for rutile at 60% dense with the P-V points calculated from known initial density, measured input stress, and measured wave velocity using conservation of momentum and mass relationships.

The risetime of the propagated wave is sufficiently long to require different methods of analysis, the wave velocity from toe-to-toe, and half max-to-half max.

Table I. Summary of time-resolved shock compression experiments

| Experiment number <sup>A</sup> | Input Condition <sup>B</sup> | Config-uration <sup>C</sup> | Input Stress <sup>D</sup> (GPa) | Wave Velocity <sup>E</sup> (km/s) | Prop. Risetime <sup>F</sup> (nsec) | Output Stress <sup>G</sup> (GPa) | Relative Volume <sup>H</sup> | $V_o$ |
|--------------------------------|------------------------------|-----------------------------|---------------------------------|-----------------------------------|------------------------------------|----------------------------------|------------------------------|-------|
| 2496 (a)                       | 0.231                        | 2                           | 0.21                            | 1.344 (1.182)                     | 916 (400)                          | 0.32 TPX                         | 1.674 (1.649)                | 1.760 |
| 2474 (a)                       | 0.420                        | 1                           | 1.29                            | 1.964 (1.822)                     | 490 (194)                          | 1.98 Kel-F                       | 1.477 (1.440)                | 1.706 |
| 2479 (a)                       | 0.704                        | 1                           | 3.02                            | 2.099 (1.998)                     | 382 (132)                          | 3.68 Kel-F                       | 1.223 (1.176)                | 1.676 |
| BE055 (b)                      | TNT                          | 3                           | 5.10                            | 2.293 (2.132)                     | 348 (116)                          | 5.11 Kel-F                       | 1.035 (0.935)                | 1.671 |
| 2471 (a)                       | 1.045                        | 1                           | —                               | 2.514 (2.407)                     | 234 (94)                           | 6.52 Kel-F                       | —                            | 1.662 |
| BE061 (b)                      | Comp-B                       | 3                           | 6.10                            | 2.313 (2.138)                     | 300 (132)                          | 6.08 Kel-F                       | 0.925 (0.796)                | 1.684 |

A: (a) impact loading; (b) explosive loading; B: symmetric impact velocity (km/s) Cu > Cu or explosive type; C: configuration, (nominal thickness): 1: Cu(6.35mm)/Kel-F(125 $\mu$ m)/PVDF(25 $\mu$ m)/Kel-F(125 $\mu$ m)/TiO<sub>2</sub>(4mm)/Kel-F(125 $\mu$ m)/PVDF(25 $\mu$ m)/Kel-F(0.74mm)/Cu(9.52mm); 2: Cu(6.35mm)/TPX(9.4mm)/PVDF(25 $\mu$ m)/FEP(25 $\mu$ m)/TiO<sub>2</sub>(4mm)/FEP(25 $\mu$ m)/PVDF(25 $\mu$ m)/TPX(9.40mm)/Cu(6.35mm); 3: P-040/explosive(25.4mm)/Cu(12.7mm)/Cu(6.35mm)/Kel-F(125 $\mu$ m)/PVDF(25 $\mu$ m)/Kel-F(125 $\mu$ m)/TiO<sub>2</sub>(4mm)/Kel-F(125 $\mu$ m)/PVDF(25 $\mu$ m)/Kel-F(0.74mm)/Cu(9.52mm) D: PVDF measurement E: wave speed toe-to-toe(half max-to-half max) F: Propagated wave toe-to-peak(10-90%) G: PVDF measurements (in polymer backing material) H: calculated from PVDF input stress and toe-to-toe wave speed(half max-to-half max wave speed)

For the toe-to-toe measurement, the transit times are chosen from the current-versus-time data as the leading edge of the pulse referred to as time=0 in Figure 1. For half max-to-half max measurement, the time at which the current returns to the baseline is taken to be the time and level of propagated stress, from which the time at half max stress is chosen. The solid and open symbols indicate toe-to-toe and half max-to-half max calculations respectively. The high pressure work of Bugaeva covers the stress range from 20.2 to 192 GPa for 60% dense rutile with the 20.2 GPa data point shown in the upper left corner.

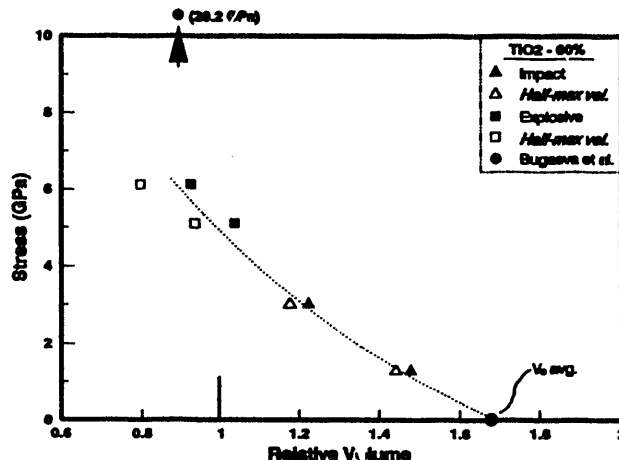


Figure 3. Measured stress-versus-relative volume states for 60% dense TiO<sub>2</sub>, using toe-to-toe and half max-to-half max wave speeds in calculations represented with solid and open symbols respectively

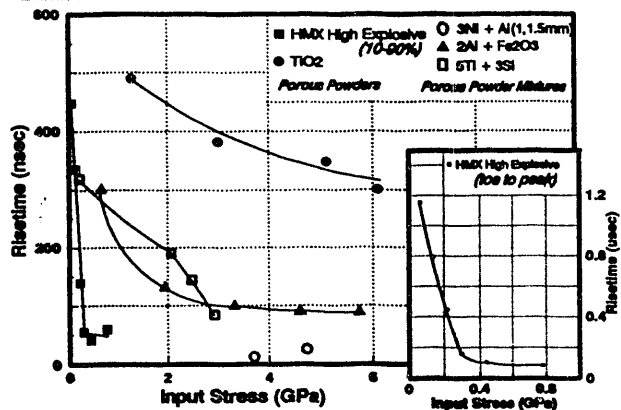


Figure 4. The 4 mm propagated wave risetime-versus-input stress is shown for five different material systems. Strongly material-dependent response is observed.

The risetime-versus-input stress relationship of the propagated wave through 4 mm thick samples is shown for four different highly porous powder systems in Figure 4. The single component systems rutile and HMX high explosive<sup>10</sup>, the unreactive two component systems, 2Al + Fe<sub>2</sub>O<sub>3</sub><sup>8</sup> and 3Ni + Al, and the reactive two component system STi + 3Si<sup>11</sup>.

The HMX has long risetimes at low stress followed by a rapid decrease in risetime due to the low crush-strength, and the onset of reaction. Rutile demonstrates a more constant trend of risetime decrease with increasing stress and a very high crush-strength without the effects of reaction. The 2Al + Fe<sub>2</sub>O<sub>3</sub> mixture exhibits a rapid decrease in risetime due to the aluminum crush-up followed by very little risetime decrease due to the Fe<sub>2</sub>O<sub>3</sub> crush-up. The STi + 3Si mixture crush-strength is initially similar to 2Al + Fe<sub>2</sub>O<sub>3</sub> followed by decrease in risetime due to reaction. The 3Ni + Al mixture show 13 and 26 nanosecond risetimes for 1.5 and 1mm sample thicknesses respectively.

#### DISCUSSION & CONCLUSION

The shock-compression of rutile shows a pressure-versus-volume relationship that crushes toward solid density in the pressure range of the present study, and shows good agreement with existing high pressure work. The propagated wave risetimes show a consistent trend of increasing inversely with input stress.

The rutile, HMX, 2Al + Fe<sub>2</sub>O<sub>3</sub>, 3Ni + Al, and STi + 3Si data illustrate the strongly material-dependent risetime characteristics which appear to be both morphologically and material dependent.

Properly packaged PVDF provide recording times of 6 microseconds, and unusual sensitivity to details while measuring stress-rate profiles.

The data provide a significant data base on materials behavior adequate for the advanced modeling required to realistically describe shock compression loading of porous solids.

#### ACKNOWLEDGEMENTS

The authors would like to acknowledge the fabrication support of Heidi Anderson and the explosive firing site support at New Mexico Tech. Supported by the U.S. Department of Energy under contract number DE-AC04-76DP00789.

#### REFERENCES

1. R. A. Graham, Solids under High Pressure Shock Compression: Mechanics, Physics and Chemistry, Springer-Verlag (1993).
2. V. A. Bugaeva, M. A. Podurets, G. V. Simakov, G. S. Telegin and R. F. Trunin, "The dynamic compressibility and equations of state of rutile-structure minerals", in *Izvestiya, Academy of Sciences, USSR, Physics of the Solid Earth*, Vol. 15, No. 1, 1979, pp.19-25.
3. R. A. Graham and N. N. Thadhani, "Solid State Reactivity of Shock-Processed Solids", in *Shock Waves in Materials Science*, edited by A. B. Sawaoka, Springer-Verlag (1993).
4. N. N. Thadhani, "Shock-Induced Chemical Reactions and Synthesis of Materials", *Progress in Materials Science*, 37, 117-226, 1993.
5. R. A. Graham, B. Morosin, Y. Horie, E. L. Venturini, M. Boslough, M. J. Carr, and D. L. Williamson, "Chemical Synthesis Under High Pressure Shock Loading", in *Shock Waves in Condensed Matter*, edited by Y. M. Gupta, Plenum (1986) pp 693-711.
6. R. A. Graham, M. U. Anderson, Y. Horie, S-K. You, and G. T. Holman, "Pressure Measurements in Chemically Reacting Powder Mixtures with the Bauer Piezoelectric Polymer Gauge", *Shock Waves*, in press.
7. R. A. Graham, M. U. Anderson, F. Bauer, and R. E. Setchell, "Piezoelectric Polarization of the Ferroelectric Polymer PVDF from 10 MPa to 10 GPa: Studies of Loading-Path Dependence", *Shock Compression of Condensed Matter - 1991*, eds. S. C. Schmidt, et al, North-Holland, (1992), pp 883-886.
8. G. T. Holman Jr., R. A. Graham, M. U. Anderson, present proceedings, in press.
9. D. E. Wackerbarth, M. U. Anderson, R. A. Graham, SAND92-0046, February, 1992, Sandia National Laboratories.
10. S. A. Sheffield, R. L. Gustavsen, R. R. Alcon, R. A. Graham, M. U. Anderson, present proceedings, in press.
11. E. W. Dunbar, R. A. Graham, M. U. Anderson, G. T. Holman Jr., N. N. Thadhani, present proceedings, in press.

## **DISCLAIMER**

This report was prepared as an account of work sponsored by an agency of the United States Government. Neither the United States Government nor any agency thereof, nor any of their employees, makes any warranty, express or implied, or assumes any legal liability or responsibility for the accuracy, completeness, or usefulness of any information, apparatus, product, or process disclosed, or represents that its use would not infringe privately owned rights. Reference herein to any specific commercial product, process, or service by trade name, trademark, manufacturer, or otherwise does not necessarily constitute or imply its endorsement, recommendation, or favoring by the United States Government or any agency thereof. The views and opinions of authors expressed herein do not necessarily state or reflect those of the United States Government or any agency thereof.

**FEND**

**DATE  
FILMED**

**11/02/93**

